$\mathcal{H}_\infty$ optimization of an integral force feedback controller

G. Zhao[1] ⓘ, A. Paknejad[1], A. Deraemaeker[2] and C. Collette[1,3]

Abstract
This paper studies the performance of the classical integral force feedback (IFF) controller for suppressing the forced response of a single degree of freedom (SDOF) system. An $\mathcal{H}_\infty$ optimization criterion is used to derive the optimal feedback gain of the IFF controller contributed as a complement for the state of the art. This optimal gain is calculated in the closed-form based on a SDOF system which is then applied to a two degrees of freedom system to study its adaptability. It is found that the $\mathcal{H}_\infty$ optimal gain can be easily transposed into multi-degrees of freedom applications without introducing too many errors. An equivalent mechanical model is also developed to enable a straightforward interpretation of the physics behind the IFF controller.

Keywords
Integral force feedback, $\mathcal{H}_\infty$, optimization, closed-form

1. Introduction

In order to meet the increasing demand for fuel efficiency, lightweight materials are more and more considered in the construction of system structures especially in the fields of aerospace engineering, robotics, and vehicle applications (Cole and Sherman, 1995; Wang and Gao, 2003; Darecki et al., 2011). However, vibrations within these systems are often lightly damped, which may easily become a major factor limiting their performance. During the past few decades, the potential of using active damping systems (Preumont, 2011) has thus been extensively explored, where additional actuators and sensors are employed and the resultant control force is formed to be proportional to the structure velocity in order to increase the structural damping. A wide range of control techniques such as integral force feedback (IFF) (Preumont et al., 1992, 2016), direct velocity feedback (Balas, 1979; Alujević et al., 2014), and positive position feedback (Fanson and Caughey, 1990) have been proposed to implement such active damping systems. One common feature of these active damping controllers is that they are relatively easy to implement, where not much prior knowledge of the system is required. However, it should be stressed that these controllers are only effective around the resonances in contrast with model-based controllers such as linear–quadratic

regulator (Borrelli and Keviczky, 2008), LMI (Chilali and Gahinet, 1996), or inverse dynamics based controllers (Wang and Xie, 2009), which may exhibit higher performance but the stability is not absolutely guaranteed.

On the other hand, it was demonstrated in Preumont et al. (1992) that active damping systems can be made unconditionally stable using IFF controllers for the collocated actuator–sensor configuration given that the time delay or the hysteresis of the actuator is negligible. One important design concern with such a control system is how the control gain of the feedback loop should be set to optimally damp the vibration of the host structure. The most widely used optimization criterion for designing an IFF controller was proposed in Preumont et al. (2016), which is referred to as the maximum damping criterion. With this technique, the

[1]Precision Mechatronics Laboratory, Beams Department, Université Libre de Bruxelles, Belgium
[2]BATir Department, Université Libre de Bruxelles, Belgium
[3]Precision Mechatronics Laboratory, Department of Aerospace and Mechanical Engineering, University of Liège, Belgium

Corresponding author:
Guoying Zhao, Université Libre de Bruxelles, Avenue F.D. Roosevelt 50, Brussels 1050, Belgium.
Email: nudt.guoying@gmail.com

optimal feedback gain is sought to obtain the most achievable damping for one specified structural mode. In this context, the damping is mainly introduced to reduce the setting time of the transient response to impulsive disturbances. Similarly, the function of damping can be also interpreted to reduce the amplitude of the forced response in the vicinity of the resonances.

This work builds upon the IFF control strategy and proposes a new optimal tuning law based on the $\mathcal{H}_\infty$ optimization criterion. Accordingly, the optimal gain is set to minimize the maximum steady state response of the structure. The presented optimal tuning law is preferred when the system is being continuously disturbed, for example, in the applications of the facilities dedicated to experimental physics (Meimon et al., 2010; Collette et al., 2013; Sivo et al., 2014). The optimal feedback gain under the $\mathcal{H}_\infty$ optimization criterion is firstly derived in a closed-form formulation for a single degree of freedom (SDOF) system and then for a two Degrees of freedom (TDOF) system. In this way, the performance degradation of applying the optimal tuning law derived for the SDOF system to the TDOF system is investigated. It is found that the $\mathcal{H}_\infty$ optimal gain derived with the SDOF system can be easily transposed into a TDOF system application using only the modal information without introducing too many errors.

The paper is structured into four sections: in Section 2, a SDOF system is presented, based on which the $\mathcal{H}_\infty$ optimal feedback gain is derived; Section 3 investigates the relative errors due to the approximations when applying the optimal feedback gain derived in Section 2 into a TDOF system; and Section 4 draws the conclusions.

2. Mathematical model and ∞ optimization

The system under investigation is shown in Figure 1(a). The structure is modeled as an undamped, lumped parameter SDOF system, defined through the mass m_1 and the stiffness k_1. It is excited by a disturbance force F. A force actuator with its stiffness of k_a is placed in parallel to the passive mount and a force sensor is mounted between the actuator and the structure to capture the force delivered by the actuator to the mass. The control loop is implemented by feeding the integral of the force sensor output denoted by F_s with a negative amplification gain back to drive the actuator which generates the control force $F_a = -g \int_0^t F_s \mathrm{d}t$.

The governing equations of the system read

$$m_1 \ddot{x} + k_1 x = F + F_s \tag{1}$$

$$F_s = -g \int_0^t F_s \mathrm{d}t - k_a x \tag{2}$$

where g is the feedback gain.

Transforming equations (1) and (2) to the Laplace domain, the driving point receptance of the system can be derived

$$\frac{x}{F} = \frac{g + s}{m_1 s^3 + g m_1 s^2 + (k_1 + k_a)s + g k_1} \tag{3}$$

where s is Laplace variable.

The magnitude of the frequency response of the driving point receptance is taken as the performance index and it is given by

$$\left| \frac{x}{F} \right| = \frac{\sqrt{g^2 + \omega^2}}{\sqrt{\begin{array}{c} m_1^2 \omega^6 + m_1(g^2 m_1 - 2k_1 - 2k_a)\omega^4 \\ + \left(k_1^2 + (-2g^2 m_1 + 2k_a)k_1 + k_a^2\right)\omega^2 + g^2 k_1^2 \end{array}}} \tag{4}$$

where ω is circular frequency.

In order to obtain a straightforward interpretation of the physics behind the IFF, an equivalent mechanical model is developed with an identical dynamical behavior as the system shown in Figure 1 (a). This mechanical model is depicted in Figure 1(b); the effectiveness of applying IFF is equivalent to having a dashpot in series with the actuator spring. This damping coefficient is feedback gain dependent which is given by

$$d_a = \frac{k_a}{g} \tag{5}$$

In the case where $g = 0$ (corresponding to no control), there is no relative displacement over d_a such that k_a represents the whole actuator branch. On the other hand when $g = \infty$, the branch which contains d_a breaks such that no transmission force passes this branch and the whole actuator effect disappears resulting in the softening effect of using IFF. The equivalent mechanical model as shown in Figure 1 (b) is actually known as a relaxation damper (Marneffe et al., 2009). One interesting point of a relaxation damper, is that all the driving point receptances with different damping to stiffness ratios will cross each other at a fixed point. Analogically to the fixed- point theory proposed in Den Hartog (1985) to design a tuned mass damper (TMD), it is natural to consider that the optimal damping to stiffness ratio of the relaxation damper is achieved when the response at the fixed point corresponds to the maximum of the driving point receptance. This process is actually called $\mathcal{H}_\infty$ optimization.
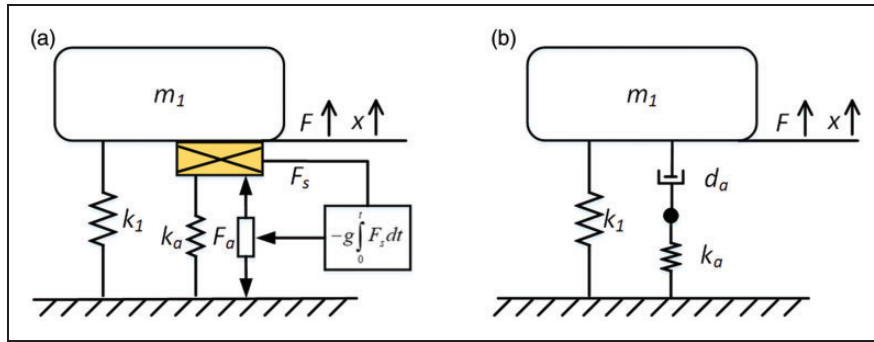
Figure 1. (a) scheme of the system under investigation; and (b) mechanical replacement model.

In the following part of this section, the optimal gain of the IFF controllers is derived in the closed-form under $\mathcal{H}_\infty$ criterion. Equation (4) is taken as the performance index. The optimal value of g to minimize the maximum of the performance index is derived by solving the following equations for g and ω

$$\frac{\partial \left|\frac{x}{F}\right|}{\partial g} = 0 \tag{6}$$

$$\frac{\partial \left|\frac{x}{F}\right|}{\partial \omega} = 0 \tag{7}$$

or:

$$gk_a\omega^2\left(-2m_1\omega^2 + 2k_1 + k_a\right) = 0 \tag{8}$$

$$-m_1^2\omega^6 - 2m_1\left(g^2m_1 - \frac{k_1 + k_a}{2}\right)\omega^4$$
$$- g^2m_1\left(g^2m_1 - 2(k_1 + k_a)\right)\omega^2 \tag{9}$$
$$+ g^2\left(g^2k_1m_1 - \left(k_1 + \frac{k_a}{2}\right)ka\right) = 0$$

Then the optimal feedback gain g_{opt} and the fixed point ω_{fixed} are calculated as

$$g_{opt} = \sqrt{\frac{\omega_o^2 + \Omega_0^2}{2}} \tag{10}$$

$$\omega_{fixed} = \sqrt{\frac{\omega_o^2 + \Omega_0^2}{2}} \tag{11}$$

where $\omega_0 = \sqrt{\frac{k_1}{m_1}}$ and $\Omega_0 = \sqrt{\frac{k_1+k_a}{m_1}}$ are the resonance frequencies of the system when the feedback gain is set to ∞ and 0, respectively. In other words, ω_0 and Ω_0 correspond to the resonance frequency of the system when the force sensor is removed and installed, respectively.

It should be noted that the optimal gain as given in equation (10) is derived provided that the primary structure is undamped. Therefore, it might not be applicable if this assumption does not hold. However, it is foreseen that the derived tuning could still guarantee an adequate approximation to the actual optimal value if the primary structure is lightly damped. In practice, the determination of the optimal gain for a damped primary structure can be achieved by an iterative procedure, and the derived optimal tuning corresponding to the undamped primary structure could be considered as a good first guess.

It is also noted that the derived ω_{fixed} as given by equation (11) is taken as the quadratic mean of the two resonance frequencies. At this particular frequency, the performance index is not invariant of the feedback gain g. The optimal gain g_{opt} is thus set to maximize the index at the fixed-point frequency, so that the response at this point becomes the maximum. In other words, the maximum performance index is minimized with the optimal feedback gain.

The effect of using IFF control is illustrated on an example system where the mass m_1 is set to $1\,\mathrm{kg}$, the stiffness $k_1 = 400\,\pi^2\mathrm{N/m}$ and the actuator stiffness $k_a = 200\,\pi^2\mathrm{N/m}$. Figure 2 shows the performance index plotted against frequency which is normalized to the fixed-point frequency as given in equation (11) for five different gain ratios defined as g/g_{opt}: 0, 1/4, 1, 4, and ∞. It is shown that all the curves intersect at a fixed point which corresponds to ω_{fixed} and only with the optimal feedback gain g_{opt} the response at the fixed point becomes the maximum in the whole frequency range. The original undamped system with no control ($g = 0$) becomes undamped again when the control gain is set to infinity.

In addition, one should also notice that the system becomes dynamically softer with the application of IFF control, meaning that the actuator does not contribute to the static stiffness of the system when the control gain is set to the values other than zero. Marneffe (2007) and Preumont et al. (2016) reported to use a high pass filter to compensate the static stiffness, which however would result in the invalidity of the
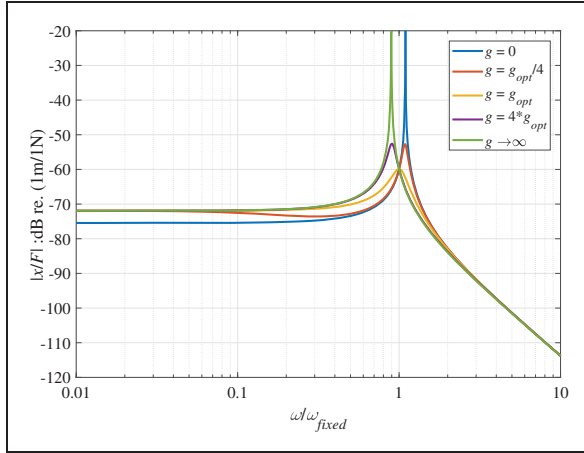
Figure 2. The magnitude of the driving point receptance plotted against the normalized frequency under different feedback gains.

Figure 3. The ratio of the optimal gain derived from the $\mathcal{H}_\infty$ and the maximum damping methods against the stiffness ratio.

derived optimal feedback gain and the compromise of the unconditional stability. Further investigations will be a subject of future work.

It is also interesting to investigate the dependence of the minimal maximum of the performance index, which can be done by substituting equation (10) into equation (4), yielding to

$$\left|\frac{x}{F}\right|_{\max} = \frac{1}{\sqrt{m_1^2\left(\frac{\Omega_0^2-\omega_0^2}{2}\right)^2}} = \frac{2}{k_a} \tag{12}$$

The expression as given in equation (12) is of particular interest as it is directly shown that this minimal maximum is inversely proportional to only one parameter, that is, the stiffness of the actuator k_a. This is because the optimal value of the performance index is determined by the product of the mass of the primary structure and the difference of the two resonance frequencies, thereby the parameters associated with the primary structure, that is, the mass m_1 and the stiffness k_1 do not play a role in determining the optimal value of the performance index. Therefore, a stiffer actuator should be chosen in the design phase in order to enhance the control performance. However, it should be argued that much more force will be then transmitted through the actuator which might be not favored in practice because of the potential failure problem.

In the following, the difference of the optimal gains derived from the $\mathcal{H}_\infty$ criterion and the maximum damping criterion are studied. The optimal gain for achieving the maximum damping is given as (Preumont et al., 2016)

$$g_{opt}^d = \Omega_i\sqrt{\frac{\Omega_i}{\omega_i}} \tag{13}$$

where ω_i and Ω_i correspond to the resonance frequency associated with the ith mode of the system when the force sensor is removed and installed, respectively.

Figure 3 plots the ratio of the optimal feedback gain derived from the $\mathcal{H}_\infty$ optimal method and that from maximum damping against the stiffness ratio between the actuator and the primary structure. It can be seen that the difference between the two optimal gains increases with the stiffness ratio. The resultant control performance associated with the two optimal settings is also studied. Two stiffness ratios $k_a/k_1 = 0.1$ and $k_a/k_1 = 1$ are considered. The corresponding optimal control gain is calculated as given in equation (10) and equation (13), respectively. Figure 4 (a) plots the performance index for the $\mathcal{H}_\infty$ optimization criterion, that is, steady state response of the driving point receptance, and Figure 4 (b) depicts the performance index for the maximum damping criterion, that is, settling time of the transient response of the primary structure to impulse disturbances. As can be seen, there is almost no difference between the two optimal tuning methods when the stiffness ratio is set to 0.1. On other hand, a visible difference in terms of the steady state response and the setting time is observed when the stiffness ratio is equal to unity. This is because when the stiffness ratio is small, the control authority with IFF is low such that the optimal gains derived from different optimal methods are similar; while when the ratio is large, different optimal gains will be set to satisfy different criteria, and the difference between the optimal gains derived from the $\mathcal{H}_\infty$ criterion and the maximum damping criterion is more pronounced.

3. Robustness of the optimal tuning law

In Section 2, the optimal feedback gain as given in equation (10) is derived for a SDOF, which can be
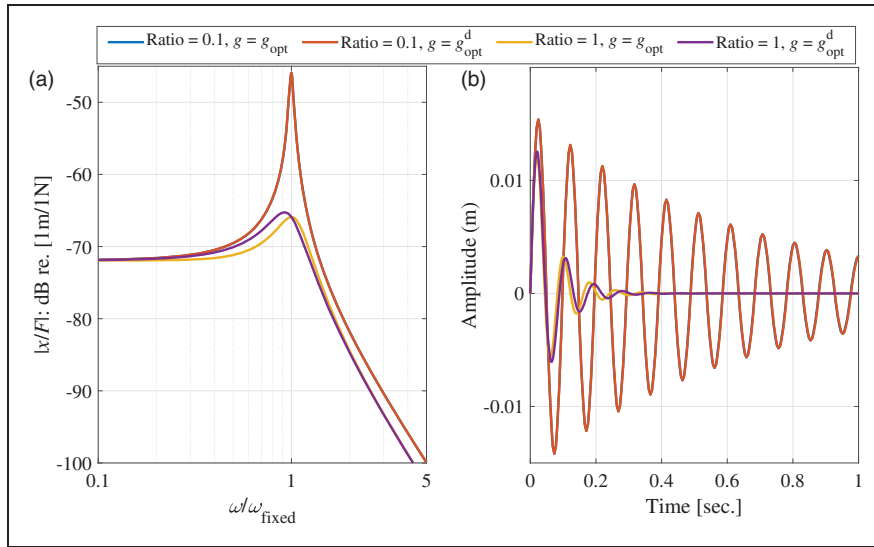
Figure 4. (a) magnitude of the driving point receptance plotted against the normalized frequency for two optimal tunings when the stiffness ratio is set to 0.1 and 1, respectively; and (b) impulse response of the system when the optimal settings are applied.

also directly applied to multi-degrees of freedom (multi-DOF) systems with well separated modes in a manner analogous to classical TMDs (Den Hartog, 1985) or piezoelectric shunts (Hagood and von Flotow, 1991; Zhao et al., 2015). For example, this can be done by performing a modal analysis of the system to calculate the natural frequencies of each mode when the actuator is installed and removed, respectively. The corresponding values are then substituted into equation (10) to obtain the optimal gain for each individual mode. However, it is not clear whether equation (10) is still valid for multi-DOF systems with closely located modes.

A TDOF undamped system as depicted in Figure 5 is thus employed to study the adaptability of the optimal gain given in equation (10). The additional mass-spring pair m_2 and k_2 acts as a vibration neutralizer and its resonance frequency in this study is set to the resonance of the lower mass-springs pair m_1 and $k_1 + k_a$, whereby the distance between the two modes of the system is mainly determined by the mass ratio between m_2 and m_1. In the following, the exact optimal gain for each vibration mode will be firstly derived and the resulting performance will be compared to that with the estimated optimal gains derived in equation (10).

The governing equations of the system read

$$m_1\ddot{x}_1 + k_1x_1 + k_2(x_1 - x_2) = F + F_s \qquad (14)$$

$$m_2\ddot{x}_2 - k_2(x_1 - x_2) = 0 \qquad (15)$$

$$F_s = -g\int_0^t F_s \mathrm{d}t - k_a x_1 \qquad (16)$$
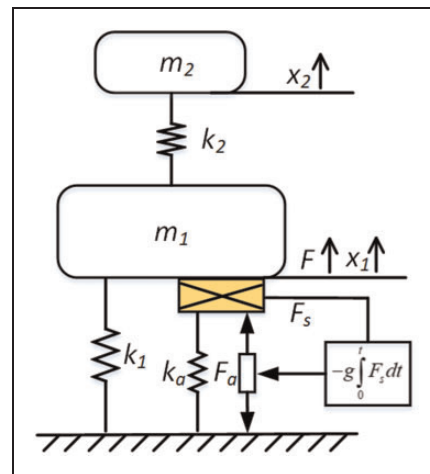
Figure 5. The scheme of two degrees of freedom system with integral force feedback control.

Transforming equations (14), (15), and (16) to a Laplace domain the driving point receptance of the system can be derived

$$\frac{x_1}{F} = \frac{(m_2s^2 + k_2)(s + g)}{\left\{ \begin{array}{l} (m_1s^2 + k_1)(s + g)(m_2s^2 + k_2) \\ + k_2m_2s^2(s + g) + k_a(m_2s^2 + k_2) \end{array} \right\}} \qquad (17)$$

where s is Laplace variable.

The magnitude of the frequency response of the driving point receptance as given in equation (17) is taken as the performance index and it is given by

$$\left|\frac{x_1}{F}\right| = \frac{\left|-m_2\omega^2 + k_2\right|\sqrt{g^2 + \omega^2}}{\sqrt{\left(\begin{array}{c}m_1m_2\omega^4 + k_2k_1 + \\ ((-m_1 - m_2)k_2 - k_1m_2)\omega^2\end{array}\right)^2 g^2 + \left(\begin{array}{c}m_1m_2\omega^4 + k_2(k_1 + k_a) + \\ ((-m_1 - m_2)k_2 - m_2(k_1 + k_a))\omega^2\end{array}\right)^2 \omega^2}} \tag{18}$$

where ω is circular frequency.

In a manner analogous to the fixed point theory (Den Hartog, 1985), two fixed points (except for the anti-resonance) would exist for a system as described in equation (18), meaning that the magnitude of the frequency response of the driving point receptance as given in equation (18) with different feedback gains will intersect at two invariable frequency locations. The frequencies at which the fixed points occur can be calculated by differentiating equation (18) with respect to the feedback gain g, and equating the derivative to zero, yields

$$\omega_{fix1} = \frac{\sqrt{-\sqrt{\begin{array}{c}4(k_1 + k_2 + 1/2k_a)^2m_2^2 + 4k_2^2m_1^2 \\ -8k_2(k_1 - k_2 + 1/2k_a)m_1m_2\end{array}} + (2k_1 + 2k_2 + k_a)m_2 + 2k_2m_1}}{2\sqrt{m_1}\sqrt{m_2}} \tag{19}$$

$$\omega_{fix2} = \frac{\sqrt{\sqrt{\begin{array}{c}4(k_1 + k_2 + 1/2k_a)^2m_2^2 + 4k_2^2m_1^2 \\ -8k_2(k_1 - k_2 + 1/2k_a)m_1m_2\end{array}} + (2k_1 + 2k_2 + k_a)m_2 + 2k_2m_1}}{2\sqrt{m_1}\sqrt{m_2}} \tag{20}$$

Substituting equation (19) and equation (20) into the partial derivative of equation (18) with respect to ω as $\partial\left|\frac{x_1}{F}\right|/\partial\omega$ respectively and solving the resulting equations for the feedback gain g, the exact optimal gain for each mode can be then derived as

$$g_{exa1} = \sqrt{\frac{\sqrt{\frac{2\left(\begin{array}{c}16P^4m_2^2 - 32P^2m_1k_2Qm_2 \\ +16m_1^2k_2^2(k_2^2 + (k_1 + 1/2k_a)^2)\end{array}\right)\sqrt{P^2m_2^2 - 2m_1k_2Qm_2 + m_1^2k_2^2}}{-32(P^2m_2 - m_1k_2Q)P(P^2m_2^2 - 2m_1k_2Qm_2 + m_1^2k_2^2)}}}{2m_1\sqrt{\frac{2(4P^2m_2^2 - 8m_1k_2(k_1 + 1/2k_a)m_2 + 4m_1^2k_2^2)\sqrt{P^2m_2^2 - 2m_1k_2Qm_2 + m_1^2k_2^2}}{-8(Pm_2 - m_1k_2)(P^2m_2^2 - 2m_1k_2Qm_2 + m_1^2k_2^2)}}}} \tag{21}$$

$$g_{exa2} = \sqrt{\frac{\sqrt{\frac{2\left(\begin{array}{c}16P^4m_2^2 - 32P^2m_1k_2Qm_2 + \\ +16m_1^2k_2^2(k_2^2 + (k_1 + 1/2k_a)^2)\end{array}\right)\sqrt{P^2m_2^2 - 2m_1k_2Qm_2 + m_1^2k_2^2}}{+32(P^2m_2 - m_1k_2Q)(k_1 + k_2 + 1/2k_a)(P^2m_2^2 - 2m_1k_2Qm_2 + m_1^2k_2^2)}}}{2m_1\sqrt{\frac{2(4P^2m_2^2 - 8m_1k_2(k_1 + 1/2k_a)m_2 + 4m_1^2k_2^2)\sqrt{P^2m_2^2 - 2m_1k_2Qm_2 + m_1^2k_2^2}}{+8(Pm_2 - m_1k_2)(P^2m_2^2 - 2m_1k_2Qm_2 + m_1^2k_2^2)}}}} \tag{22}$$

where $P = k_1 + k_2 + \frac{1}{2}k_a$ and $Q = k_1 - k_2 + \frac{1}{2}k_a$.

Applying the optimal tuning law derived in Section 2 for the SDOF system to the TDOF system under consideration, the estimated optimal gain for the ith mode ($i \in [1, 2]$) is given as

$$g_{esti} = \sqrt{\frac{\omega_{0i}^2 + \Omega_{0i}^2}{2}} \tag{23}$$

where ω_{0i}, Ω_{0i} ($i \in [1, 2]$) represents the resonance frequency of the ith mode of the system when the force sensor is removed and installed respectively and they are given by

$$\omega_{01} = \frac{\sqrt{2}\sqrt{-\sqrt{(m_1 + m_2)^2k_2^2 - 2k_1m_2(m_1 - m_2)k_2 + k_1^2m_2^2} + (m_1 + m_2)k_2 + k_1m_2}}{2\sqrt{m_1}\sqrt{m_2}} \tag{24}$$

$$\omega_{02} = \frac{\sqrt{2}\sqrt{\sqrt{(m_1+m_2)^2k_2^2 - 2k_1m_2(m_1-m_2)k_2 + k_1^2m_2^2} + (m_1+m_2)k_2 + k_1m_2}}{2\sqrt{m_1}\sqrt{m_2}} \tag{25}$$

$$\Omega_{01} = \frac{\sqrt{2}\sqrt{-\sqrt{\begin{array}{c}(k_1+k_2+k_a)^2m_2^2 + k_2^2m_1^2 \\ -2k_2m_1(k_1-k_2+k_a)m_2\end{array}} + (k_1+k_2+k_a)m_2 + k_2m_1}}{2\sqrt{m_1}\sqrt{m_2}} \tag{26}$$

$$\Omega_{02} = \frac{\sqrt{2}\sqrt{\sqrt{\begin{array}{c}(k_1+k_2+k_a)^2m_2^2 + k_2^2m_1^2 \\ -2k_2m_1(k_1-k_2+k_a)m_2\end{array}} + (k_1+k_2+k_a)m_2 + k_2m_1}}{2\sqrt{m_1}\sqrt{m_2}} \tag{27}$$

The control effectiveness with the exact gains as given in equations (21)–(22) and the estimated gains in equation (23) are compared for two cases: (1) the well separated modes case where the mass ratio m_2/m_1 is set to 0.5 and the stiffness k_2 is set according to $k_2 = (k_1 + k_a)m_2/m_1$; and (2) the closely located modes case where the mass ratio m_2/m_1 is 0.001 and the stiffness k_2 is adapting the same accordingly. The other parameters m_1, k_1 and k_a remain the same as defined in Figure 1(a).

Figure 6 compares the resulting driving point receptance with six different gains, $g = 0$, ∞, g_{est1}, g_{exa1}, g_{est2} and g_{exa2} for the well separated modes case, while Figure 7 shows the comparison for the closely located modes case. In both cases, the response at the undamped resonances is substantially suppressed and the local minimal maxima for the first and second modes are obtained when the feedback gain is set to the exact optimal parameter as given in equation (21) and equation (22), respectively. One can also see that the resultant performance index difference associated with the exact parameters and the estimated parameters is almost negligible as the corresponding curves targeted for the same mode almost coincide with each other. The obtained results indicate that the derived optimal feedback gain under $\mathcal{H}_\infty$ optimization remains, to a very large extent, an accurate estimation of the exact values even when the two modes are very close to each other.

Next, the relative errors between the gain approximations and their exact counterparts in terms of the mass ratio m_2/m_1 and the stiffness ratio k_a/k_1 are investigated. The mass ratio mainly determines the distance between the two resonances and the stiffness ratio mainly determines the IFF control performance.

Figure 8 (a) and Figure 8 (b) plot the relative feedback gain errors between the exact optimal values and the estimated values against the mass ratio and the stiffness ratio targeted for the first and the second modes, respectively. It can be shown that an increase of the relative gain errors introduced by the approximations comes with an increase in the stiffness ratio. However, the relative gain errors do not change proportionally with respect to the mass ratio, and instead there is a mass ratio near which the relative errors are maximized. Nevertheless, the relative gain errors introduced by the approximations are below 6% up to the frequency ratios from 10% to 1000%, and the mass ratio is from 0.1% to 100%.

Figure 9 (a) and Figure 9 (b) plot the relative resultant performance index errors associated with the exact optimal values and the estimated values against the mass ratio and the stiffness ratio targeted for the first and the second modes, respectively. One can see that the relative resultant performance errors introduced by the approximations are smaller than that of the relative gain errors, which is below 0.6% for the first mode and 0.03% for the second mode. The results shown by the plots indicate that the approximation as given in equation (23) is reasonable to be used to represent its exact solution in a relatively large range.

On the other hand, the IFF control performance for the TDOF system under the optimal feedback gains derived by the maximum damping criterion (Preumont et al., 2016) is also compared for the two cases. For each mode, the optimal gain for achieving the maximum damping of mode i ($i \in [1, 2]$) can be estimated as (Preumont et al., 2016)

$$g_{esti}^* = \Omega_{0i}\sqrt{\frac{\Omega_{0i}}{\omega_{0i}}} \tag{28}$$

Figure 10 (a) compares the resultant root loci with the estimated optimal parameter for each mode in the case where the two modes are well separated, while Figure 10 (b) shows the comparison for the closely located modes case. It is shown in Figure 10 (a) that the achieved damping value with the estimated optimal
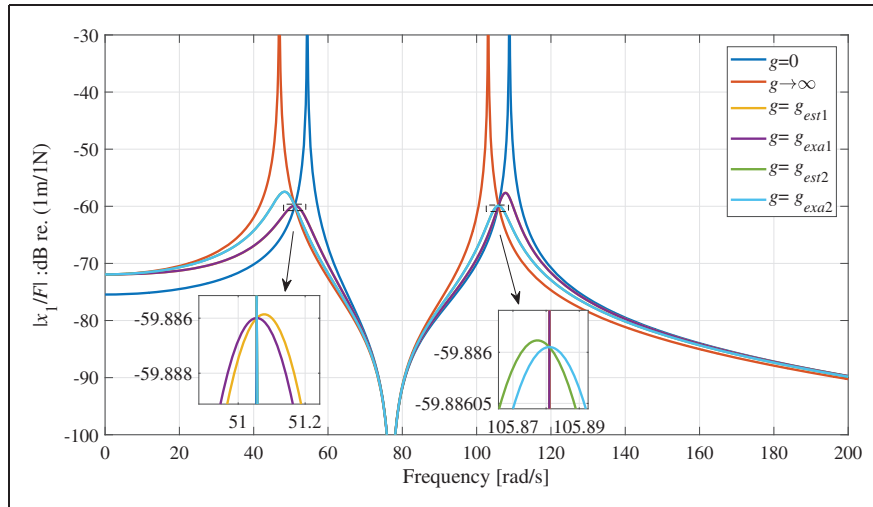
Figure 6. Comparison of the driving point receptance under different feedback gains for the well separated modes case.
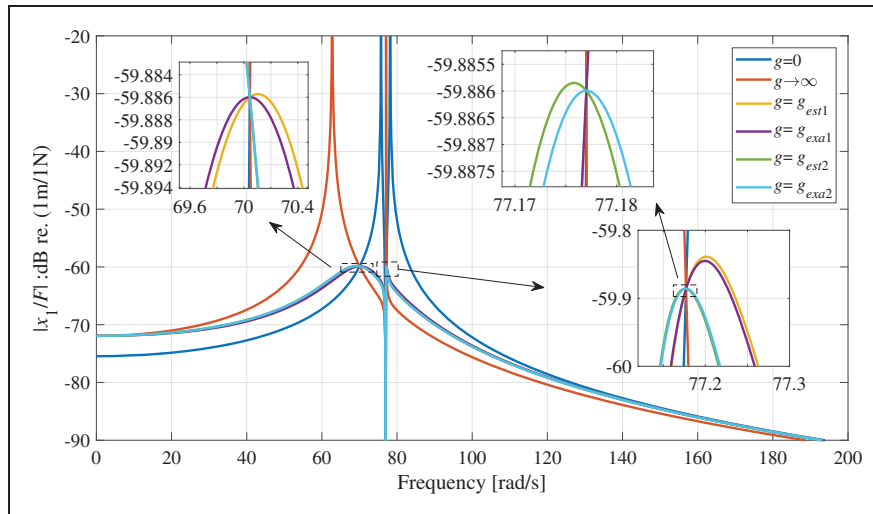
Figure 7. Comparison of the driving point receptance under different feedback gains for the closely located modes case.
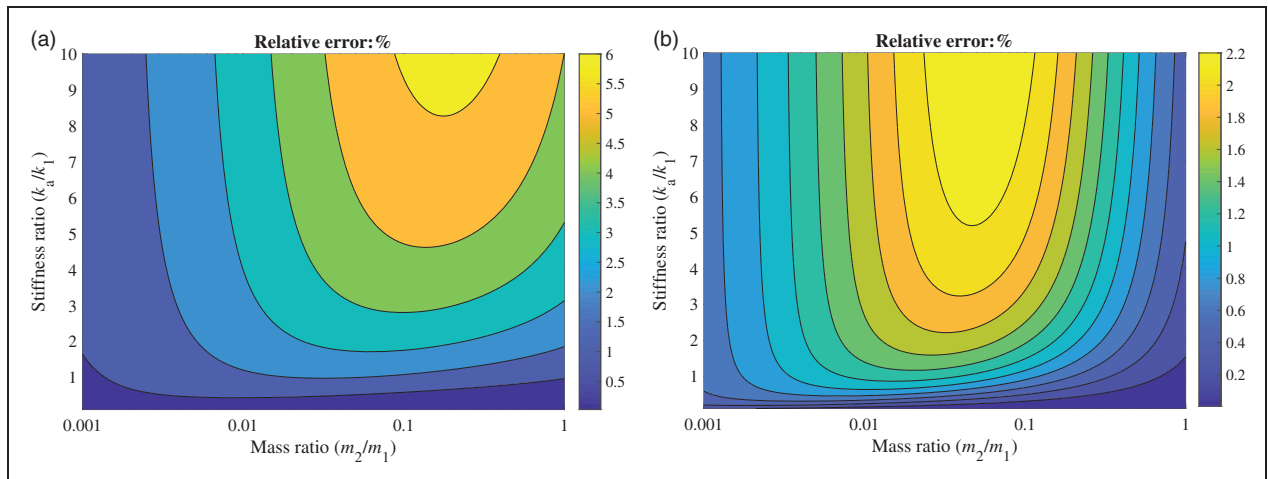
Figure 8. The relative errors of the feedback gains for: (a) first mode; and (b) second mode.
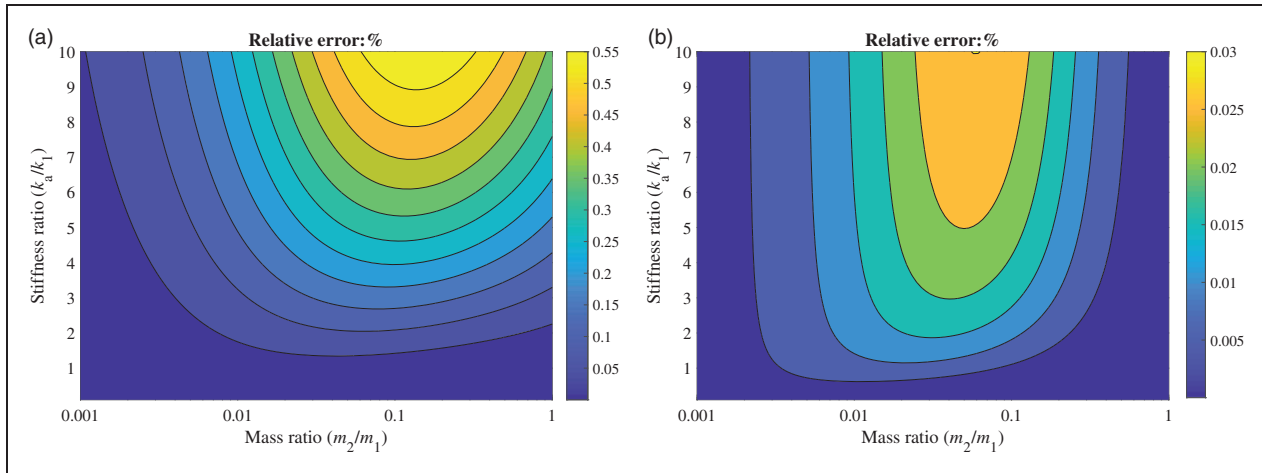
Figure 9. The relative errors of the performance index for: (a) first mode; and (b) second mode.
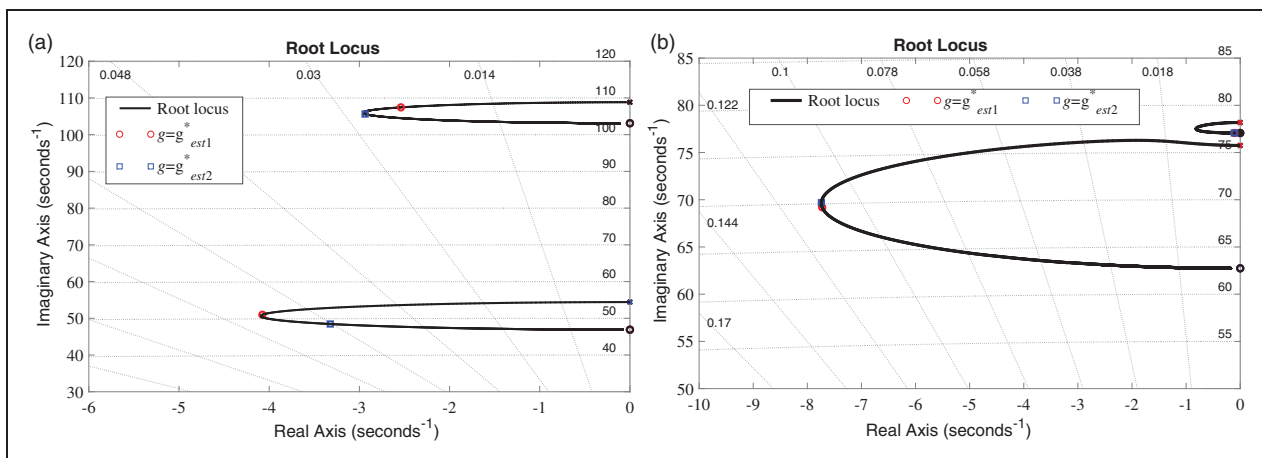
Figure 10. Root locus with the integral force feedback controller for: (a) well separated case; and (b) closely located case.

parameter for each mode is very well graphically approaching to the corresponding maximum achieved damping, meaning that the estimated optimal parameter is a reasonable approximation to its exact value when the modal modes are well separated. However, on the contrary, there is a relatively large error for the optimal gain approximation for the second mode in terms of the resultant achieved damping for the case when the modes are closely located. This indicates that the optimal parameter derived with the maximum damping criterion may suffer from the restriction of the location of the poles of the system.

4. Conclusions

This paper studies the performance of the classical IFF controller for suppressing the forced response of a SDOF system. The $\mathcal{H}_\infty$ optimization criterion is used to derive the optimal feedback gain of the IFF

controller contributed as a complement for the state of the art. This optimal gain is calculated in the closed-form based on a SDOF system which is then applied to a TDOF system to study its adaptability. It is found that the $\mathcal{H}_\infty$ optimal gain can be easily transposed into m-DOF applications without introducing too many errors. An equivalent mechanical model is also developed to enable a straightforward interpretation of the physics behind the IFF controller.

ORCID iD

G. Zhao https://orcid.org/0000-0001-6967-7341

References

Alujević N, Zhao G, Depraetere B, et al. (2014) H2 optimal vibration control using inertial actuators and a comparison with tuned mass dampers. *Journal of Sound and Vibration* 333(18): 4073–4083.

Balas MJ (1979) Direct velocity feedback control of large space structures. *Journal of Guidance, Control, and Dynamics* 2(3): 252–253.

Borrelli F and Keviczky T (2008) Distributed LQR design for identical dynamically decoupled systems. *IEEE Transactions on Automatic Control* 53(8): 1901–1912.

Chilali M and Gahinet P (1996) H ∞ design with pole placement constraints: An LMI approach. *IEEE Transactions on Automatic Control* 41(3): 358–367.

Cole GS and Sherman AM (1995) Light weight materials for automotive applications. *Materials Characterization* 35(1): 3–9.

Collette C, Tshilumba D, Fueyo-Rosa L, et al. (2013) Conceptual design and scaled experimental validation of an actively damped carbon tie rods support system for the stabilization of future particle collider superstructures. *Review of Scientific Instruments* 84(2): 1–8.

Darecki M, Edelstenne C, Enders T, et al. (2011) Flightpath 2050. Flightpath 2050 Europe's Vision for Aviation. Brussels: European Commission. Available at https://ec.europa.eu/transport/sites/transport/files/modes/air/doc/flightpath2050.pdf

Den Hartog JP (1985) *Mechanical Vibrations*. New York: Dover Publications.

Fanson JL and Caughey TK (1990) Positive position feedback control for large space structures. *AIAA Journal* 28(4): 717–724.

Hagood NW and von Flotow A (1991) Damping of structural vibrations with piezoelectric materials and passive electrical networks. *Journal of Sound and Vibration* 146(2): 243–268.

Marneffe B De (2007) Active and passive vibration isolation and damping via shunted transducers. PhD Thesis. Université Libre de Bruxelles. Available at: http://scmero.ulb.ac.be/Publications/Thesis/de_Marneffe07.pdf (accessed 6 January 2014).

Marneffe B De, Avraam M, Deraemaeker A, et al. (2009) Vibration isolation of precision payloads: A six-axis electromagnetic relaxation isolator. *Journal of Guidance, Control, and Dynamics* 32(2): 395–401.

Meimon S, Petit C, Fusco T, et al. (2010) Tip–tilt disturbance model identification for Kalman-based control scheme: Application to XAO and ELT systems. *Journal of the Optical Society of America, A: Optics, Tmage Science, and Vision* 27(11): A122–A132.

Preumont A (2011) *Vibration Control of Active Structures: An Introduction*, 2nd edition. Dordrecht: Kluwer Academic.

Preumont A, Dufour J-P and Malekian C (1992) Active damping by a local force feedback with piezoelectric actuators. *Journal of Guidance, Control, and Dynamics* 15(2): 390–395.

Preumont A, Voltan M, Sangiovanni A, et al. (2016) Active tendon control of suspension bridges. *Smart Structures and Systems* 18(1): 31–52.

Sivo G, Kulcsár C, Conan J-M, et al. (2014) First on-sky SCAO validation of full LQG control with vibration mitigation on the CANARY pathfinder. *Optics Express* 22(19): 23565.

Wang F-Y and Gao Y (2003) *Advanced Studies of Flexible Robotic Manipulators: Modeling, Design, Control and Applications*. Singapore: World Scientific.

Wang H and Xie Y (2009) Adaptive inverse dynamics control of robots with uncertain kinematics and dynamics. *Automatica* 45(9): 2114–2119.

Zhao G, Alujević N, Depraetere B, et al. (2015) Dynamic analysis and $\mathcal{H}_\infty$ optimisation of a piezo-based tuned vibration absorber. *Journal of Intelligent Material Systems and Structures* 26(15): 1995–2010.